DOI:10.1021/jf904179m

JOURNAL OF AGRICULTURAL AND FOOD CHEMISTRY
ARTICLE

Protein Molecular Structures and Protein Fraction Profiles of New Coproducts from BioEthanol Production: A Novel Approach

Peiqiang Yu,* Zhiyuan Niu, and Daalkhaijav Damiran

College of Agriculture and Bioresources, University of Saskatchewan, 51 Campus Drive, Saskatoon, SK, Canada S7N 5A8

The objectives of this study were to determine the protein molecular structures of the new coproducts from bioethanol production, quantify protein structure amide I to II and α-helix to β-sheet spectral peak intensity ratio, and illustrate multivariate molecular spectral analyses as a novel research tool for rapid characterization of protein molecular structures in bioethonal bioproducts. The study demonstrated that the grains had a significantly higher ratio of α-helix to β-sheet in the protein structure than their coproducts produced from bioethanol processing (1.38 vs 1.03, $P < 0.05$). There were significant differences between wheat and corn (1.47 vs 1.29, $P < 0.05$) but no difference between wheat dried distiller grains with solubles (DDGS) and corn DDGS (1.04 vs 1.03, $P > 0.05$). The grains had a significantly higher ratio of protein amide I to II in the protein structure than their coproducts produced from bioethanol processing (4.58 vs 2.84, $P < 0.05$). There were no significant differences between wheat and corn (4.61 vs 4.56, $P > 0.05$), but there were significant differences between wheat DDGS and corn DDGS (3.08 vs 2.21, $P < 0.05$). This preliminary study indicated that bioethanol processing changes protein molecular structures, compared with original grains. Further study is needed with a large set of the new bioethanol coproducts to quantify protein molecular structures (α-helix to β-sheet ratio; amide I to II ratio) of the bioethanol coproducts in relation to nutrient supply and availability in animals.

KEYWORDS: Protein molecular structures; α-helix to β-sheet ratio; amide I to II ratio; coproducts from bioethanol production

INTRODUCTION

The dramatic increase in bioethanol production in North America has resulted in million tons and different types of new coproducts: wheat dried distillers grains with solubles (DDGS), corn DDGS, and blend DDGS (e.g., wheat/corn = 70:30; 50:50; 20:80). A systematical study on chemical, mineral, and nutrient profiles of these new coproducts of bioethanol production has been reported recently by Nuez-Ortín and Yu (*1*). The animal performances in chicken, pigs, beef, and dairy cattle fed the coproducts from bioethanol production at different levels have been studied (*2*−*5*). But none of published studies in literature reported what type of changes occurred in the molecular structure of the new bioethanol coproducts after bioethanol processing, compared with those in original grains. None of the published studies in the literature reported how the molecular structure changes were associated with nutrient availability in the rumen and intestine and total nutrient supply to dairy cattle. Molecular structures of proteins (the second structures) include mainly α-helices and β-sheets and small amounts of β-turns and random coils (*6*, *7*). Studying these structure profiles of proteins leads to an understanding of the components that make up a whole protein. The protein structure profiles may affect access by gastrointestinal digestive enzymes and influence protein functionality, quality, and nutrient availability or protein digestive behavior (*8*−*12*). The objectives of this study were to (1) determine the changes in the molecular structures of proteins of these new coproducts from bioethanol production; (2) quantify the protein structure amide I to II ratio and the α-helix to β-sheet ratio; and (3) illustrate the multivariate molecular spectral analyses as a novel research tool for rapid characterization of protein molecular structures.

MATERIALS AND METHODS

New Coproducts from Bioethanol Production. Total six co-products from bioethanol production: wheat DDGS, blend DDGS (wheat/corn = 70:30), and corn DDGS as well as original feedstock wheat and corn grains were collected. The detailed results and discussion on the effects of bioethanol plant and DDGS type with a large sample data set on chemical characteristics, protein, and carbohydrate subfraction profiles, energy values, and rumen disappearance at 24 and 48 h of incubation were reported (*1*).

Fourier Transformed Infrared Spectroscopy. Each sample of the new coproducts from bioethanol production was finely ground three times to pass through a 250 μm screen (Retsch ZM-1, Brinkmann

*Corresponding author. College of Agriculture and Bioresources, University of Saskatchewan 6D10 Agriculture Building, 51 Campus Drive, Saskatoon, SK, Canada, S7N 5A8. Tel: +1 306 966 4132. E-mail: peiqiang.yu@usask.ca.

 Published on Web 02/24/2010

Table 1. Protein Molecular Structural Characteristics of Amides I and II and Their Ratios: Comparison between Different Grains (Wheat and Corn) and Different Types of DDGS [Wheat DDGS, Corn DDGS, and Blend DDGS (Wheat/Corn = 70:30)] from Bioethanol Production, Revealed Using DRIFT Molecular Spectroscopy[a]

		protein amide I and amide II[b]		
items	number of repetitions for DRIFT analysis	amide I	amide II	ratio of amide I to amide II
Amides IR peak center position		~1655 cm^{-1}	~1550 cm^{-1}	~1655/~1550 cm^{-1}
Amides IR peak region		Ca. 1720−1575 cm^{-1}	Ca. 1575−1485 cm^{-1}	
Amides IR peak area baseline		Ca. 1720−1485 cm^{-1}	Ca. 1720−1485 cm^{-1}	Ca. 1720−1485 cm^{-1}
			based on the protein amide I and II peak area	
feeds				
wheat (grain)	8	162.45 b	35.14 b	4.61 a
corn (grain)	8	64.42 c	14.15 b	4.56 a
wheat DDGS	16	291.79 a	95.03 a	3.08 b
corn DDGS	8	261.81 a	118.45 a	2.21 c
blend DDGS	8	274.68 a	92.03 a	2.97 b
SEM[c]		26.663	9.262	0.059
			P value	
statistics				
feeds		<0.0001	0.0013	0.0129
grain vs bioethanol coproducts				
grain	16	113.44 b	24.64 b	4.58 a
DDGS	32	280.02 a	100.13 a	2.84 b
SEM		17.923	6.237	0.076
			P value	
statistics				
grain and bioethanol coproducts		<0.0001	<0.0001	<0.0001

[a] Means with the different letters in the same column differ, $P < 0.05$. [b] The protein amide data unit: IR absorbance unit. Protein peak baseline: 1720 to 1485 cm^{-1}. Protein amide I area region: 1720 to 1575 cm^{-1}. Protein amide II area region: 1575 to 1485 cm^{-1}. [c] SEM = pooled standard error of means.

Instruments (Canada) LTD, Ontario). Samples of the ground new coproducts were then mixed with KBr in a ratio of 1 part of coproduct with 4 parts of KBr in a 2 mL centrifuge tube and mixed by vortex for 10 s. Diffuse reflectance infrared Fourier transform spectroscopy (DRIFT) was performed using a Bio-Rad FTS-40 with a ceramic IR source and MCT detector (Bio-Rad laboratories, Hercules, California, USA). Data was collected using Win-IR software. Spectra were generated from the mid-IR (4000−800 cm^{-1}) portion of the electromagnetic spectrum with 256 coadded scans and a spectral resolution of 4 cm^{-1}.

Molecular Spectral Analysis of Protein. Molecular spectral analysis was done with OMNIC 7.2 software (Spectra Tech., USA). Protein amides I and II and protein secondary structures α-helix and β-sheet were identified according to published reports (*9*, *13*−*17*).

Quantifying Amides I and II and α-Helix and β-Sheet Spectral Peak Intensity Ratios in Protein Structures. The protein IR spectrum has two primary features. The protein amide I bond is primarily a C═O stretching vibration (80%) plus C−N stretching vibration (*14*, *15*). Protein amide I absorbs at ca. 1655 cm^{-1}. Protein amide II which absorbs at ca. 1550 cm^{-1} consists primarily of N−H bending vibrations (60%) coupled with C−N stretching vibrations (40%) (*14*, *15*). The amide I and II absorption intensity of the peak area and their ratio were calculated with baseline at ca.1720−1485 cm^{-1}.

The vibrational frequency of the protein amide I band is particularly sensitive to protein secondary structure (*9*, *13*−*16*) and can be used to predict protein secondary structures. For the α-helix, protein amide I is typically in the range of ca. 1648−1660 cm^{-1}. For the β-sheet, the peak can be found within the range of ca. 1625−1640 cm^{-1}. Amide II is also used to assess protein conformation. However, as it arises from complex vibrations involving multiple functional groups, it is less useful for protein structure prediction than the amide I band (*14*).

To estimate the peak intensity of the α-helix and β-sheet of the protein molecular structures, two steps were applied. Briefly, the first step used Fourier self-deconvolution (FSD: a method for resolving intrinsically overlapped bands) and the second derivative function in OMNIC 7.2 to obtain the FSD and second derivative spectra in the protein amide I region at ca. 1720−1575 cm^{-1} and then identified the protein amide I component peak frequencies. The detailed concepts and algorithm of FSD were described by Kauppinen et al. (*18*) and Griffths and Pariente (*19*). The second step was to quantify the intensity of the peak height of the α-helix and β-sheet and their ratio (*20*).

Statistical Analysis. Statistical analyses were performed using the MIXED procedure of SAS (version 9.1.3). The model used for the analysis was $Y_{ij} = \mu + T_i + e_{ij}$, where Y_{ij} was an observation of the dependent variable ij (amide I, amide II, α-helix, β-sheet, and their ratios); μ was the population mean for the variable; T_i was the different feeds, as a fixed effect, and e_{ij} was the random error associated with the observation ij. The contrast statement was used to compare grains and DDGS samples.

For all statistical analyses, significance was declared at $P < 0.05$ and trends at $P \leq 0.10$. Differences among the treatments were evaluated using a multiple comparison test following the Fisher's Protected LSD method.

Multivariate Molecular Spectral Analysis for DRIFT Spectra. Multivariate molecular spectral analyses, principal component analysis (PCA), and hierarchical cluster analysis (CLA) were performed using Statistica software 6.0 (StatSoft Inc., Tulsa, OK, USA) to classify and distinguish between the inherent structures.

RESULTS AND DISCUSSION

Detecting Changes in Protein Molecular Structure Amide I to Amide II Ratio by Bioethanol Processing. The amide I and II profile depends on the protein molecular structure and may be

Table 2. Characteristics of Protein Secondary Structure (α-Helix, β-Sheet, and Their Ratio): Comparison between Different Grains (Wheat and Corn) and Different Types of DDGS [Wheat DDGS, Corn DDGS, and Blend DDGS (Wheat/Corn = 70:30)] from Bioethanol Production, Revealed Using DRIFT Molecular Spectroscopy[a]

					protein secondary structures[b]		
		infrared absorption			α-helix	β-sheet	ratio of α-helix to β-sheet
items	number of repetitions for DRIFT analysis	α-helix peak center (cm^{-1})	β-sheet peak center (cm^{-1})	peak baseline (cm^{-1})	~1655 cm^{-1}	~1630 cm^{-1}	~1655/~1630 cm^{-1}
					based on the protein α-helix and β-sheet peak height		
feeds							
wheat	8	1658	1629	~1724−1485	2.25 b	1.53 b	1.47 a
corn	8	1658	1627	~1724−1489	0.90 c	0.70 b	1.29 b
wheat DDGS	16	1660	1628	~1730−1485	3.38 a	3.22 a	1.04 c
corn DDGS	8	1658	1626	~1724−1484	3.25 a	3.14 a	1.03 cd
blend DDGS	8	1659	1628	~1726−1487	3.02 ab	3.02 a	0.99 d
SEM[c]					0.329	0.300	0.013
						P value	
statistics							
feeds					<0.0001	<0.0001	<0.0001
grain vs coproducts							
grains	16	1658	1627	~1724−1485	1.57 b	1.11 b	1.38 a
DDGS	32	1659	1628	~1724−1485	3.26 a	3.15 a	1.03 b
SEM[c]					0.225	0.195	0.014
						P value	
statistics							
grain and coproducts					<0.0001	<0.0001	<0.0001

[a] Means with the different letters in the same column differ, $P < 0.05$. [b] The protein amide data unit: IR absorbance unit. [c] SEM = pooled standard error of means.

affected by processing methods. Recent medical research shows that compared with normal tissue, diseased tissues (such as Prion tissue and cancer tissue) result in a change of percentage of protein secondary structure and/or a reduced ratio of amide I to amide II (*21*, *22*). Protein amide I (ca. 1720−1575 cm^{-1}) and amide II (ca. 1575−1485 cm^{-1}) bands arise from specific stretching and bending vibrations of the protein backbone (*14*, *15*). Their profiles are usually used to reveal protein molecular structure.

In food, feed, and nutrition research, to date, little has been done on the relationship of the protein molecular structure amide I and II profiles and their ratios to nutritive value. **Table 1** shows the molecular structural characteristics of protein amide I and II and their ratios. Compared to the grains, the new coproducts from bioethanol production had significantly different amide profiles ($P < 0.05$) with higher amide I and II but lower protein structure amide I to II ratio (2.84 vs 4.58, $P < 0.05$). There were no significant differences between wheat and corn (4.61 vs 4.56, $P > 0.05$), but significantly different amide profiles between wheat DDGS and corn DDGS (3.08 vs 2.21, $P < 0.05$) were present. These results indicated that bioethanol processing changes the original grain protein molecular structural chemical makeup. The difference in the amide I to amide II profiles and their ratio may cause a difference in nutrient value (*8*−*11*, *23*).

Detecting Changes in Protein Secondary Structure Profile and α-Helix to β-Sheet Ratio by Bioethanol Processing. In the new coproducts from bioethanol production and grains, the spectrum of the protein amide I original band shows peak centers at ca. 1658 and 1628 cm^{-1}. This was confirmed from the FSD spectrum of amide I and the second derivative spectrum of amide I at the region of 1720−1575 cm^{-1}. Because protein amide I component peaks overlay each other, Fourier self-deconvolution and the second derivative function were used to obtain FSD/2nd derivative spectra (1720−1575 cm^{-1} region) to identify amide I component peak frequencies in order to quantify the protein α-helix and β-sheet peak center height in the original protein amide I region at ca. 1720−1575 cm^{-1}.

Table 2 shows the molecular structural characteristics of the protein α-helix and β-sheet and their ratios. Compared with the grains, the new coproducts from bioethanol production had significantly higher ($P < 0.05$) in the α-helix (3.26 vs 1.57) and β-sheet (3.15 vs 1.11) and lower ($P < 0.05$) in the α-helix to β-sheet ratio (1.03 vs 1.38). There were significant differences in protein secondary structure profiles (α-helix, β-sheet, and their ratio) between wheat and corn ($P > 0.05$) but no significant differences between wheat DDGS and corn DDGS ($P > 0.05$). No published results have been found for the characteristics of protein secondary structures in different new coproducts from bioethanol production; therefore, no comparison could be made.

These results indicate that these new coproducts and grains differed in protein secondary structure conformation in terms of the ratio of protein α-helix and β-sheet, indicating the differences in protein molecular structural chemical makeup and features. Bioethanol processing changes original grain protein molecular structure. These structural differences may impact the new coproducts' protein utilization and availability in the rumen and intestine in dairy cows. Our results demonstrate that the molecular spectral analytical technique to localize relatively pure protein bodies may reveal differences in the protein molecular structural chemical makeup. The different protein α-helix and β-sheet structures by altering access to gastrointestinal digestive enzymes may result in differences in protein value and protein availability (*9*, *10*, *12*, *24*).

Discriminating and Classifying Protein Molecular Structure. Cluster analysis can be used to cluster IR molecular spectra on

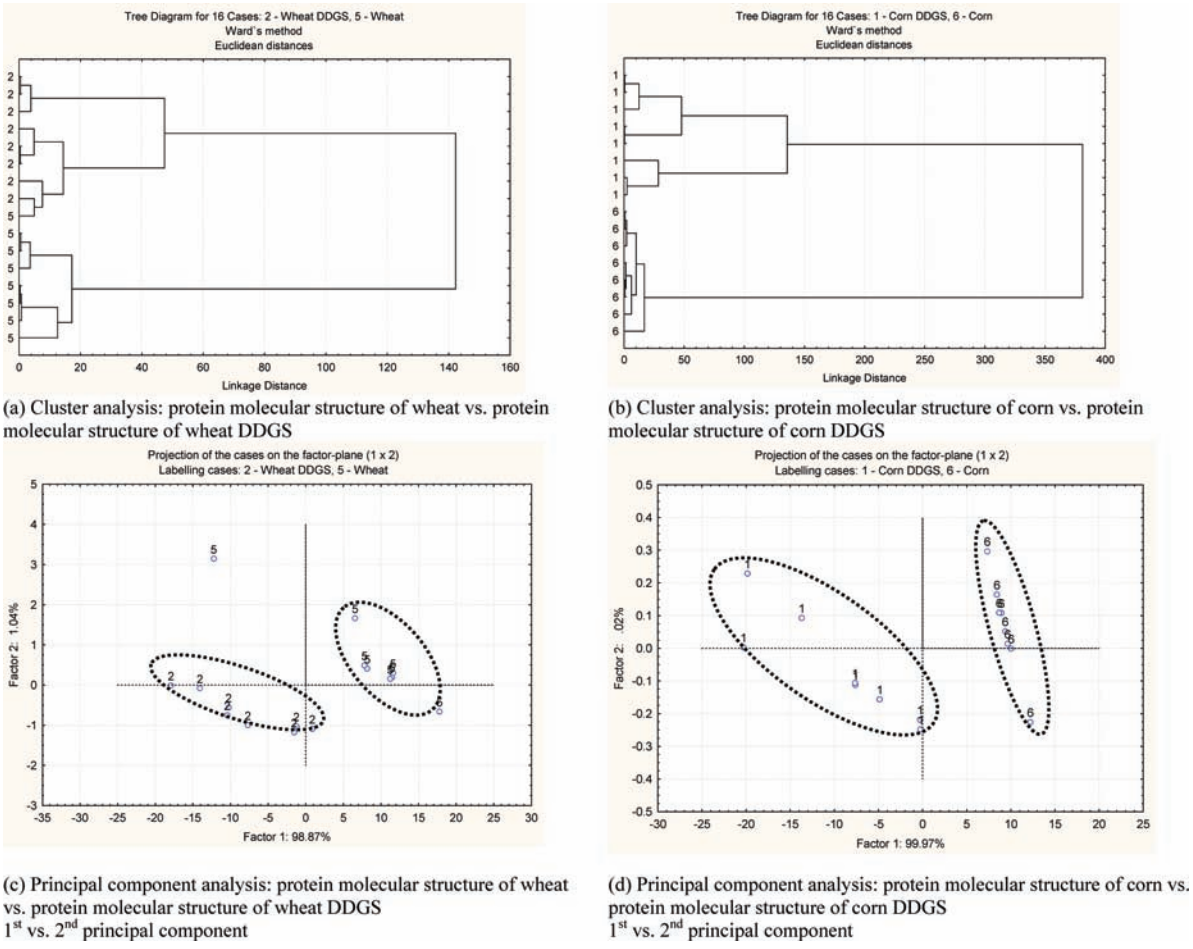

(a) Cluster analysis: protein molecular structure of wheat vs. protein molecular structure of wheat DDGS

(b) Cluster analysis: protein molecular structure of corn vs. protein molecular structure of corn DDGS

(c) Principal component analysis: protein molecular structure of wheat vs. protein molecular structure of wheat DDGS 1st vs. 2nd principal component

(d) Principal component analysis: protein molecular structure of corn vs. protein molecular structure of corn DDGS 1st vs. 2nd principal component

Figure 1. Multivariate molecular spectral analyses of protein molecular structure of the new coproducts from bioethanol production: CLA cluster analyses of the molecular spectrum of protein amides I and II (region ca. 1720−1485 cm^{-1}; distance method, Euclidean; cluster method, Ward's algorithm); PCA analyses of the molecular mid-IR spectrum of protein amides I and II. (**a**,**c**) Wheat DDGS (code 2) vs wheat (code 5); (**b**,**d**) corn DDGS (code 1) vs corn (code 6).

the basis of similarity with other spectra. In this study, the Ward's algorithm method was used without any prior parametrization of the spectral data (original protein amide I and II spectral data) in the IR region (ca. 1720−1475 cm^{-1}). This method helps discriminate the structure chemical makeup differences between the products. **Figure 1a**,**b** shows that two classes can be distinguished between wheat versus wheat DDGS and corn versus corn DDGS, indicating that the protein molecular structure between the grains and bioethanol coproducts was different.

The second multivariate analysis tested was principal component analysis (PCA), a statistical data reduction method. In this barley protein inherent structure study, PCA analysis was used to identify the main sources of variation in the protein amide I and II original spectra in the region 1720−1485 cm^{-1} of original grain and bioethanl coproducts and identify features that differed between these two.

Wheat and wheat DDGS can be grouped in separate ellipses (**Figure 1c**) with no overlapping of groups. The first three PCs individually explain 98.87, 1.04, and 0.07% of the variation in the protein amide spectrum data set. **Figure 1d** also shows that corn and corn DDGS can be grouped in separate ellipses with no overlapping of groups. The first three PCs individually explain 99.97, 0.02, and 0.01% of the variation in the protein amide spectrum data set. In both parts, the first PC can explain 99% of the total variation.

This was a preliminary study with a small data set. Future studies will be carried out on the relationship between protein molecular structures (e.g., α-helix to β-sheet ratio; amide I to II ratio) and protein profiles, subfractions, and nutrient supply and availability in new bioethanol coproducts with a large data set.

In conclusion, the study showed that the protein molecular structure of the new coproducts from bioethanol production and structural changes by bioethenol processing could be revealed and identified, on the basis of the DRIFT analytical technique. The protein structure α-helix to β-sheet ratio and amides I to II ratio were significantly different between the grains and the new coproducts from bioethanol production. Bioethanol processing might change protein molecular structures compared with those of the original grains.

LITERATURE CITED

(1) Nuez-Ortín, W. G.; Yu, P. Nutrient variation and availability of wheat DDGS, corn DDGS and blend DDGS from bioethanol plants. *J. Sci. Food Agric.* **2009**, *89*, 1754–1761.

(2) Firkins, J. L.; Berger, L. L.; Fahey, G. C., Jr. Evaluation of wet and dry distillers grains and wet and dry corn gluten feeds for ruminants. *J. Anim Sci.* **1985**, *60*, 847–860.

(3) Widyaratne, G. P.; Zijlstra, R. T. Nutrient value of wheat and corn distiller's dried grain with solubles: Digestibility and digestible contents of energy, amino acids and phosphorus, nutrient excretion and growth performance of grower-finisher pigs. *Can. J. Anim. Sci.* **2006**, *87*, 103–114.

(4) Beliveau, R. Effects of Increasing Levels of Wheat-based Dried Distiller's Grains in a Barley Ration on Growth Performance,

Carcass Quality and Rumen Fermentation Characteristics in Feedlot Steers. M.Sc. Thesis, University of Saskatchewan, Canada, **2008**.

(5) Klopfenstein, T. J.; Erickson, G. E.; Bremer, V. R. Board-invited review: Use of distillers byproducts in the beef cattle feeding industry. *J Anim Sci*. **2008**, *86*, 1223–1231.

(6) Carey, F. A. *Organic Chemistry*, 3rd ed.; McGraw-Hill Companies, Inc.: New York, 1996.

(7) Jackson, M.; Mantsch, H. H. The use and misuse of FTIR spectroscopy in the determination of protein structure. *Biochem Mol. Biol*. **1995**, *30*, 95–120.

(8) Golovina, E. A.; Wolkers, W. F.; Hoekstra, F. A. Long-term stability of protein secondary structure in dry seeds. *Comp. Biochem. Physiol., Part A: Mol. Integr. Physiol*. **1997**, *117A*, 343–348.

(9) Wetzel, D. L.; Srivarin, P.; Finney, J. R. Revealing protein infrared spectral detail in a heterogeneous matrix dominated by starch. *Vib. Spectrosc*. **2003**, *31*, 109–114.

(10) Seguchi, M.; Takemoto, M.; Mizutani, U.; Ozawa, M.; Nakamura, C.; Matsumura, Y. Effects of secondary structures of heated egg white protein on the binding between prime starch and tailings fractions in fresh wheat flour. *Cereal Chem*. **2004**, *81*, 633–636.

(11) Yu, P.; McKinnon, J. J.; Christensen, C. R.; Christensen, D. A. Using synchrotron FTIR microspectroscopy to reveal chemical features of feather protein secondary structure, comparison with other feed protein sources. *J. Agric. Food Chem*. **2004**, *52*, 7353–7361.

(12) Yu, P. Protein secondary structures (α-helix and β-sheet) at a cellular level and protein fractions in relation to rumen degradation behaviors of protein: A novel approach. *Br. J. Nutri*. **2005**, *94*, 655–665.

(13) Kemp, W. *Organic Spectroscopy*, 3rd ed.; W.H. Freeman and Company: New York, 1991.

(14) Jackson, M.; Mantsch H. H. Biomedical Infrared Spectroscopy. In *Infrared Spectroscopy of Biomolecules*; Mantsch, H. H., Chapman, D., Eds.; Wiley-Liss: New York, 1996; pp 311−340.

(15) Jackson, M.; Mantsch, H. H. Ex Vivo Tissue Analysis by Infrared spectroscopy. In *Encyclopedia of Analytical Chemistry*; Meyers, R. A., Ed.; John Widely & Sons: New York, 2000; Vol. 1, pp 131−156.

(16) Marinkovic, N. S.; Chance, M. R. Synchrotron Infrared Microspectroscopy. In *Encyclopedia of Molecular Cell Biology and Molecular Medicine*; Wiley, Inc., Hoboken, NJ, 2006; pp 2671−2708.

(17) Miller, L. M.; Dumas, P. Chemical imaging of biological tissue with synchrotron infrared light. *Biochim. Biophys. Acta* **2006**, *1757*, 846–857.

(18) Kauppinen, J. K.; Moffatt, D. J.; Mantsch, H. H.; Cameron, D. G. Fourier self-deconvolution: a method for resolving intrinsically overlapped bands. *Appl. Spectrosc*. **1981**, *35*, 271–276.

(19) Griffths, P. R.; Pariente, G. Introduction to spectral deconvolution. *Trends Anal. Chem*. **1986**, *5*, 209–215.

(20) Yu, P. Synchrotron IR microspectroscopy for protein structure analysis: potential and questions: A Review. *Spectroscopy* **2006**, *20*, 229–251.

(21) Kneippa, J.; Miller, L. M.; Joncica, M.; Kittelc, M.; Lascha, P.; Beekesa, M.; Naumanna, D. In situ identification of protein structural changes in prion-infected tissue. *Biochim. Biophy. Acta* **2003**, *1639*, 152–158.

(22) Wang, Q.; Kretlow, A.; Beekes, M.; Naumann, D.; Miller, L. In situ characterization of prion protein structure and metal accumulation in scrapie-infected cells by synchrotron infrared and X-ray imaging. *Vib. Spectrosc*. **2005**, *38*, 61–69.

(23) Yu, P.; McKinnon, J. J.; Soita, H. W.; Christensen, C. R.; Christensen, D. A. Use of synchrotron-based FTIR microspectroscopy to determine protein secondary structures of raw and heat treated brown and golden flaxseeds: A novel approach. *Can. J. Anim. Sci*. **2005**, *85*, 437–448.

(24) Doiron, K. J.; Yu, P.; McKinnon, J. J.; Christensen, D. A. Heat-induced protein structures and protein subfractions in relation to protein degradation kinetics and intestinal availability in dairy cattle. *J. Dairy Sci*. **2009**, *92*, 3319–3330.

Received for review December 1, 2009. Revised manuscript received February 4, 2010. Accepted February 6, 2010. This research has been supported by grants from the Ministry of Agriculture Strategic Research Chair Program, the Agricultural Bioproducts Innovation Program (ABIP-FOBI) of Agriculture and Agric-Food Canada (AAFC), the Saskatchewan Agricultural Development Fund (ADF), and Beef Cattle Research Council (BCRC).